1.28. Let $f(x, y)$ denote a 2-D analog function that is circularly symmetric and can therefore be expressed as

$$f(x, y) = g(r)\big|_{r=\sqrt{x^2+y^2}}.$$

Let $F(\Omega_x, \Omega_y)$ denote the 2-D analog Fourier transform of $f(x, y)$. For a circularly symmetric $f(x, y)$, $F(\Omega_x, \Omega_y)$ is also circularly symmetric and can therefore be expressed as

$$F(\Omega_x, \Omega_y) = G(\rho)\big|_{\rho=\sqrt{\Omega_x^2+\Omega_y^2}}.$$

Note that the analog case is in sharp contrast with the discrete-space case, in which circular symmetry of a sequence $x(n_1, n_2)$ does not imply circular symmetry of its Fourier transform $X(\omega_1, \omega_2)$. The relationship between $g(r)$ and $G(\rho)$ is called the *zeroth-order Hankel transform* pair and is given by

$$G(\rho) = 2\pi \int_{r=0}^{\infty} rg(r)J_0(r\rho)\, dr$$

and

$$g(r) = \frac{1}{2\pi} \int_{\rho=0}^{\infty} \rho G(\rho)J_0(r\rho)\, d\rho,$$

where $J_0(\cdot)$ is the Bessel function of the first kind and zeroth order. Determine the Fourier transform of $f(x, y)$ when $f(x, y)$ is given by

$$f(x, y) = \begin{cases} 1, & \sqrt{x^2 + y^2} \le 2 \\ 0, & \text{otherwise.} \end{cases}$$

Note that $$xJ_1(x)\big|_{x=a}^{b} = \int_{x=a}^{b} xJ_0(x)\, dx$$

where $J_1(x)$ is the Bessel function of the first kind and first order.

1.29. Cosine transforms are used in many signal processing applications. Let $x(n_1, n_2)$ be a real, finite-extent sequence which is zero outside $0 \le n_1 \le N_1 - 1$, $0 \le n_2 \le N_2 - 1$. One of the possible definitions of the cosine transform $C_x(\omega_1, \omega_2)$ is

$$C_x(\omega_1, \omega_2) = \sum_{n_1=0}^{N_1-1} \sum_{n_2=0}^{N_2-1} x(n_1, n_2) \cos \omega_1 n_1 \cos \omega_2 n_2.$$

(a) Express $C_x(\omega_1, \omega_2)$ in terms of $X(\omega_1, \omega_2)$, the Fourier transform of $x(n_1, n_2)$.

(b) Derive the inverse cosine transform relationship; that is, express $x(n_1, n_2)$ in terms of $C_x(\omega_1, \omega_2)$.

1.30. In reconstructing an image from its Fourier transform phase, we have used an iterative algorithm, shown in Figure 1.30. The method of imposing constraints separately in each domain in an iterative manner in order to obtain a solution that satisfies all the required constraints is useful in a variety of applications. One such application is the band-limited extrapolation of a signal. As an example of a band-limited extrapolation problem, consider $x(n_1, n_2)$, which has been measured only for $0 \le n_1 \le N - 1$, $0 \le n_2 \le N - 1$. From prior information, however, we know that $x(n_1, n_2)$ is band-limited and that its Fourier transform $X(\omega_1, \omega_2)$ satisfies $X(\omega_1, \omega_2) = 0$ for $\sqrt{\omega_1^2 + \omega_2^2} \ge \omega_c$. Develop an iterative algorithm that may be used for determining $x(n_1, n_2)$ for all (n_1, n_2). You do not have to show that your algorithm converges to a desired solution. However, using $N = 1$, $x(0, 0) = 1$, and $\omega_c = \frac{\pi}{2}$, carry out a few iterations of your algorithm and illustrate that it behaves reasonably for at least this particular case.

1.31. Let $x(n_1, n_2)$ represent the intensity of a digital image. Noting that $|X(\omega_1, \omega_2)|$ decreases rapidly as the frequency increases, we assume that an accurate model of $|X(\omega_1, \omega_2)|$ is

$$|X(\omega_1, \omega_2)| = \begin{cases} Ae^{-2\sqrt{\omega_1^2+\omega_2^2}}, & \sqrt{\omega_1^2 + \omega_2^2} \leq \pi \\ 0, & \text{otherwise.} \end{cases}$$

Suppose we reconstruct $y(n_1, n_2)$ by retaining only a fraction of the frequency components of $x(n_1, n_2)$. Specifically,

$$Y(\omega_1, \omega_2) = \begin{cases} X(\omega_1, \omega_2), & \sqrt{\omega_1^2 + \omega_2^2} \leq \frac{\pi}{10} \\ 0, & \text{otherwise.} \end{cases}$$

The fraction of the frequency components retained is $\frac{\pi(\pi/10)^2}{4\pi^2}$, or approximately 1%. By evaluating the quantity

$$\frac{\sum_{n_1=-\infty}^{\infty} \sum_{n_2=-\infty}^{\infty} (y(n_1, n_2) - x(n_1, n_2))^2}{\sum_{n_1=-\infty}^{\infty} \sum_{n_2=-\infty}^{\infty} x^2(n_1, n_2)}$$

discuss the amount of distortion in the signal caused by discarding 99% of the frequency components.

1.32. For a typical image, most of the energy has been observed to be concentrated in the low-frequency regions. Give an example of an image for which this observation may not be valid.

1.33. In this problem, we derive the projection-slice theorem, which is the basis for computed tomography. Let $f(t_1, t_2)$ denote an analog 2-D signal with Fourier transform $F(\Omega_1, \Omega_2)$.

(a) We integrate $f(t_1, t_2)$ along the t_2 variable and denote the result by $p_0(t_1)$; that is,

$$p_0(t_1) = \int_{t_2=-\infty}^{\infty} f(t_1, t_2)\, dt_2.$$

Express $P_0(\Omega)$ in terms of $F(\Omega_1, \Omega_2)$, where $P_0(\Omega)$ is the 1-D Fourier transform of $p_0(t_1)$ given by

$$P_0(\Omega) = \int_{t_1=-\infty}^{\infty} p_0(t_1)e^{-j\Omega t_1}\, dt_1.$$

(b) We integrate $f(t_1, t_2)$ along the t_1 variable and denote the result by $p_{\pi/2}(t_2)$; that is,

$$p_{\pi/2}(t_2) = \int_{t_1=-\infty}^{\infty} f(t_1, t_2)\, dt_1.$$

Express $P_{\pi/2}(\Omega)$ in terms of $F(\Omega_1, \Omega_2)$, where $P_{\pi/2}(\Omega)$ is the 1-D Fourier transform of $p_{\pi/2}(t_2)$ given by

$$P_{\pi/2}(\Omega) = \int_{t_2=-\infty}^{\infty} p_{\pi/2}(t_2)e^{-j\Omega t_2}\, dt_2.$$

(c) Suppose we obtain $a(t, u)$ from $f(t_1, t_2)$ by the coordinate rotation given by

$$a(t, u) = f(t_1, t_2)\big|_{t_1 = t\cos\theta - u\sin\theta,\, t_2 = t\sin\theta + u\cos\theta}$$

where θ is the angle shown in Figure P1.33(a). In addition, we obtain $B(\Omega_1', \Omega_2')$ from $F(\Omega_1, \Omega_2)$ by coordinate rotation given by

$$B(\Omega_1', \Omega_2') = F(\Omega_1, \Omega_2)\big|_{\Omega_1 = \Omega_1'\cos\theta - \Omega_2'\sin\theta,\, \Omega_2 = \Omega_1'\sin\theta + \Omega_2'\cos\theta}$$

where θ is the angle shown in Figure P1.33(b).

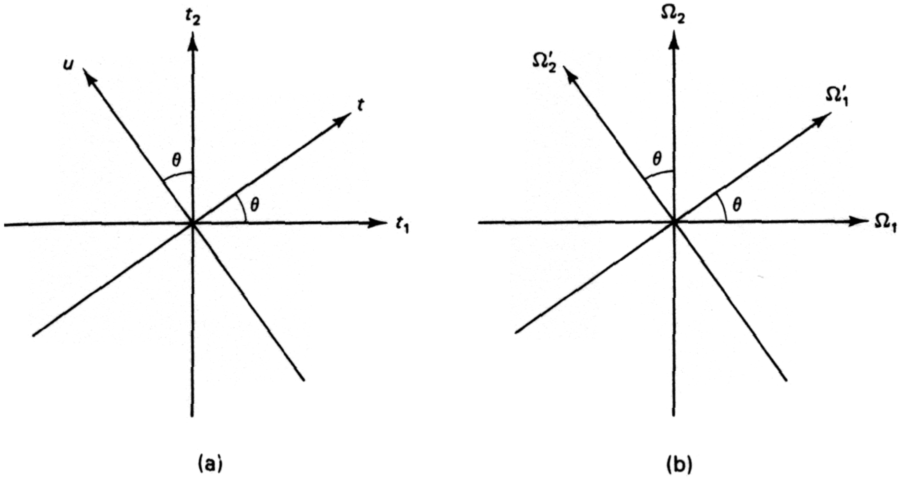

Figure P1.33

Show that $B(\Omega_1', \Omega_2') = A(\Omega_1', \Omega_2')$ where

$$A(\Omega_1', \Omega_2') = \int_{t=-\infty}^{\infty}\int_{u=-\infty}^{\infty} a(t, u)e^{-j\Omega_1' t}e^{-j\Omega_2' u}\, dt\, du.$$

The result states that when $f(t_1, t_2)$ is rotated by an angle θ with respect to the origin in the (t_1, t_2) plane, its Fourier transform $F(\Omega_1, \Omega_2)$ rotates by the same angle in the same direction with respect to the origin in the (Ω_1, Ω_2) plane. This is a property of the 2-D analog Fourier transform.

(d) Suppose we integrate $f(t_1, t_2)$ along the u variable where the u variable axis is shown in Figure P1.33(a). Let the result of integration be denoted by $p_\theta(t)$. The function $p_\theta(t)$ is called the projection of $f(t_1, t_2)$ at angle θ. Using the results of (a) and (c) or the results of (b) and (c), discuss how $P_\theta(\Omega)$ can be simply related to $F(\Omega_1, \Omega_2)$, where

$$P_\theta(\Omega) = \int_{t=-\infty}^{\infty} p_\theta(t)e^{-j\Omega t}\, dt.$$

The relationship between $P_\theta(\Omega)$ and $F(\Omega_1, \Omega_2)$ is the projection-slice theorem.

1.34. Consider an analog 2-D signal $s_c(t_1, t_2)$ degraded by additive noise $w_c(t_1, t_2)$. The degraded observation $y_c(t_1, t_2)$ is given by

$$y_c(t_1, t_2) = s_c(t_1, t_2) + w_c(t_1, t_2).$$

Suppose the spectra of $s_c(t_1, t_2)$ and $w_c(t_1, t_2)$ are nonzero only over the shaded regions shown in the following figure.

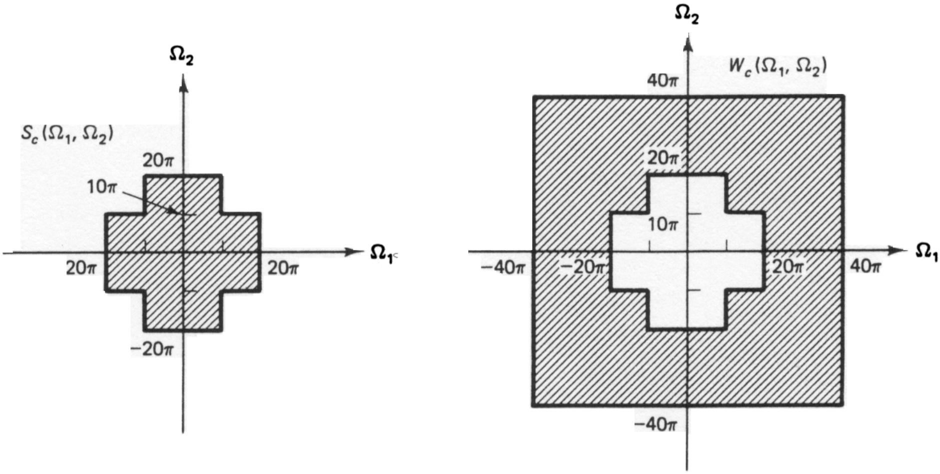

Figure P1.34

We wish to filter the additive noise $w_c(t_1, t_2)$ by digital filtering, using the following system:

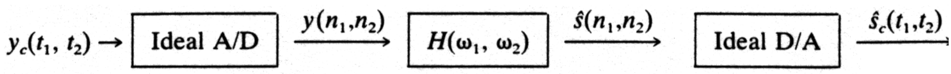

$$y(n_1, n_2) = y_c(t_1, t_2)|_{t_1 = n_1T_1, t_2 = n_2T_2}$$

$$\hat{s}_c(t_1, t_2) = \sum_{n_1=-\infty}^{\infty} \sum_{n_2=-\infty}^{\infty} \hat{s}(n_1, n_2) \frac{\sin \frac{\pi}{T_1}(t_1 - n_1T_1) \sin \frac{\pi}{T_2}(t_2 - n_2T_2)}{\frac{\pi}{T_1}(t_1 - n_1T_1) \frac{\pi}{T_2}(t_2 - n_2T_2)}$$

Assuming that it is possible to have any desired $H(\omega_1, \omega_2)$, determine the maximum T_1 and T_2 for which $\hat{s}_c(t_1, t_2)$ can be made to equal $s_c(t_1, t_2)$.

1.35. In Section 1.5, we discussed the results for the ideal A/D and D/A converters when the analog signal is sampled on a rectangular grid. In this problem, we derive the corresponding results when the analog signal is sampled on a hexagonal grid. Let $x_c(t_1, t_2)$ and $X_c(\Omega_1, \Omega_2)$ denote an analog signal and its analog Fourier transform. Let $x(n_1, n_2)$ and $X(\omega_1, \omega_2)$ denote a sequence and its Fourier transform. An ideal A/D converter converts $x_c(t_1, t_2)$ to $x(n_1, n_2)$ by

$$x(n_1, n_2) = \begin{cases} x_c(t_1, t_2)|_{t_1 = n_1T_1, t_2 = n_2T_2}, & \text{if both } n_1 \text{ and } n_2 \text{ are even, or both } n_1 \text{ and } n_2 \text{ are odd} \\ 0, & \text{otherwise.} \end{cases} \quad (1)$$

The sampling periods T_1 and T_2 are related by $T_2 = \frac{\sqrt{3}}{3} T_1$. The sampling grid used in (1) is shown in the following figure.

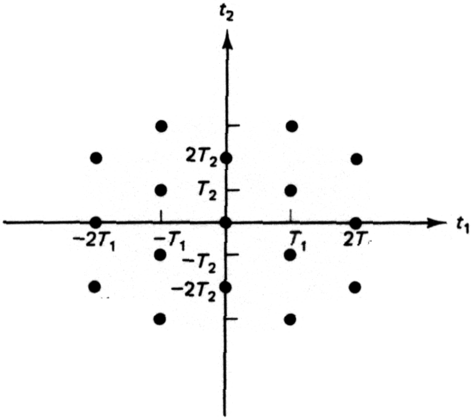

Figure P1.35a

We wish to derive the relationship between $X(\omega_1, \omega_2)$ and $X_c(\Omega_1, \Omega_2)$. It is convenient to represent (1) by the system shown below:

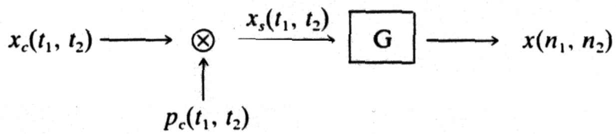

The function $p_c(t_1, t_2)$ is a periodic train of impulses given by

$$p_c(t_1, t_2) = \sum_{n_1=-\infty}^{\infty} \sum_{n_2=-\infty}^{\infty} \delta(t_1 - 2n_1T_1, t_2 - 2n_2T_2) + \sum_{n_1=-\infty}^{\infty} \sum_{n_2=-\infty}^{\infty} \delta(t_1 - 2n_1T_1 - T_1, t_2 - 2n_2T_2 - T_2) \qquad (2)$$

where $\delta(t_1, t_2)$ is a dirac-delta function. The system G converts an analog signal $x_s(t_1, t_2)$ to a sequence $x(n_1, n_2)$ by measuring the area under each impulse and using it as the amplitude of the sequence $x(n_1, n_2)$.

(a) Sketch an example of $x_c(t_1, t_2)$, $x_s(t_1, t_2)$ and $x(n_1, n_2)$. Note, from (1), that $x(n_1, n_2)$ is zero for even n_1 and odd n_2 or odd n_1 and even n_2.

(b) Determine $P_c(\Omega_1, \Omega_2)$. Note that the Fourier transform of

$$\sum_{n_1=-\infty}^{\infty} \sum_{n_2=-\infty}^{\infty} \delta(t_1 - n_1T, t_2 - n_2T)$$

is given by

$$\left(\frac{2\pi}{T}\right)^2 \sum_{r_1=-\infty}^{\infty} \sum_{r_2=-\infty}^{\infty} \delta\left(\Omega_1 - \frac{2\pi r_1}{T}, \Omega_2 - \frac{2\pi r_2}{T}\right)$$

(c) Express $X_s(\Omega_1, \Omega_2)$ in terms of $X_c(\Omega_1, \Omega_2)$.

(d) Express $X(\omega_1, \omega_2)$ in terms of $X_s(\Omega_1, \Omega_2)$.

(e) From the results from (c) and (d), express $X(\omega_1, \omega_2)$ in terms of $X_c(\Omega_1, \Omega_2)$.

(f) Using the result from (e), sketch an example of $X_c(\Omega_1, \Omega_2)$ and of $X(\omega_1, \omega_2)$.

(g) Suppose $x_c(t_1, t_2)$ is band-limited to a circular region such that $X_c(\Omega_1, \Omega_2)$ has the following property:

$$X_c(\Omega_1, \Omega_2) = 0, \qquad \sqrt{\Omega_1^2 + \Omega_2^2} \geq \Omega_c.$$

Determine the conditions on T_1 and T_2 such that $x_c(t_1, t_2)$ can be exactly recovered from $x(n_1, n_2)$.

(h) Comparing the result from (g) with the corresponding result based on using a rectangular sampling grid, discuss which sampling grid is more efficient for exactly reconstructing $x_c(t_1, t_2)$ from a smaller number of samples of $x_c(t_1, t_2)$ if $X_c(\Omega_1, \Omega_2)$ is band-limited to a circular region.

(i) Show that the sampling grid used in this problem is very efficient compared with sampling on a rectangular grid when $x_c(t_1, t_2)$ is band-limited to the hexagonal region shown below.

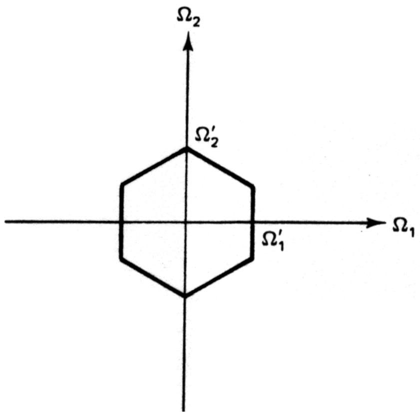

Figure P1.35b

We now derive the results for the ideal D/A converter for a hexagonal sampling grid. When $x_c(t_1, t_2)$ is sampled at a sufficiently high rate, the ideal D/A converter recovers $x_c(t_1, t_2)$ exactly from $x(n_1, n_2)$. It is convenient to represent the ideal D/A converter by the system shown below:

$$x(n_1, n_2) \longrightarrow \boxed{G^{-1}} \xrightarrow{x_s(t_1,t_2)} \boxed{H_c(\Omega_1, \Omega_2)} \xrightarrow{y_c(t_1,t_2)}$$

The system G^{-1} is the inverse of the system G discussed above.

(j) Express $x_s(t_1, t_2)$ in terms of $x(n_1, n_2)$.

(k) Determine the frequency response $H_c(\Omega_1, \Omega_2)$ such that $y_c(t_1, t_2) = x_c(t_1, t_2)$. Assume that $x(n_1, n_2)$ was obtained by sampling $x_c(t_1, t_2)$ at a sufficiently high rate on the hexagonal sampling grid.

(l) Using the results from (j) and (k), express $y_c(t_1, t_2)$ in terms of $x(n_1, n_2)$.

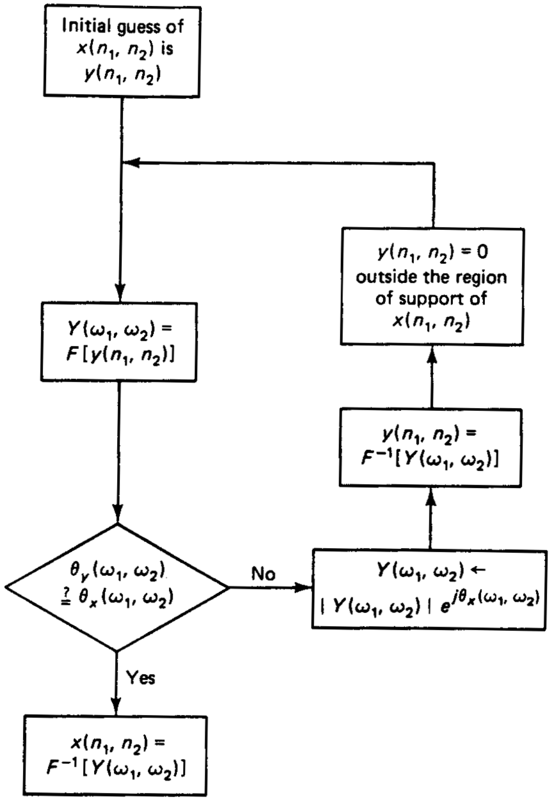

Figure 1.30 Iterative procedure for phase-only reconstruction of $x(n_1, n_2)$ from its phase $\theta_x(\omega_1, \omega_2)$.

only synthesis of (1.39)], 10 iterations, and 50 iterations. The initial estimate used is $\delta(n_1, n_2)$.

Although the magnitude-only synthesis of (1.40) does not capture the intelligibility of typical signals, almost all typical images are also uniquely specified by the Fourier transform magnitude. Specifically, if $x(n_1, n_2)$ is real, has finite extent, and has a nonfactorable Fourier transform, then $x(n_1, n_2)$ is uniquely specified by its Fourier transform magnitude $|X(\omega_1, \omega_2)|$ within a sign factor, translation, and rotation by 180 degrees [Bruck and Sodin, Hayes]. This raises the possibility of exactly reconstructing $x(n_1, n_2)$ from $|X(\omega_1, \omega_2)|$ within a sign factor, translation and rotation by 180 degrees. This is known in the literature as the *phase-retrieval* problem, and has many more potential applications than the phase-only reconstruction problem. Unfortunately, none of the algorithms developed to date are as straightforward or well-behaved as the algorithms developed for the phase-only reconstruction problem. It is possible to derive a closed-form algorithm or a set of linear equations that can be used in solving for $x(n_1, n_2)$ from $|X(\omega_1, \omega_2)|$, but their derivation is quite involved [Izraelevitz and Lim, Lane, et al.]. In addition, the closed-form solution is not practical for an image of reasonable size due to the large number of linear equations that must be solved. It is also possible to derive